Journal of Luminescence 170 (2016) 375–379

Contents lists available at ScienceDirect

Journal of Luminescence

journal homepage: www.elsevier.com/locate/jlumin

# Silk fibroin-antigenic peptides-$YVO_4$:$Eu^{3+}$ nanostructured thin films as sensors for hepatitis C

Lais R. Lima [a], Marli L. Moraes [b], Karina Nigoghossian [a], Maristela F.S. Peres [a], Sidney J.L. Ribeiro [a,*]

[a] Institute of Chemistry, São Paulo State University, UNESP, CP355, Araraquara, SP 14801-970, Brazil
[b] Institute of Science and Technology, Federal University of São Paulo, UNIFESP, São José dos Campos, SP 12231-280, Brazil

ARTICLE INFO

*Article history:*
Received 29 January 2015
Received in revised form
11 June 2015
Accepted 21 August 2015
Available online 8 September 2015

*Keywords:*
Luminescent nanoparticles
Europium
Silk fibroin
Antigenic peptide
Immunosensor

ABSTRACT

Nanostructured films prepared by Layer-by-Layer technique and containing silk fibroin, antigenic peptide NS5A-1 derived from hepatitis C virus (HCV) NS5A protein and $YVO_4$:$Eu^{3+}$ luminescent nanoparticles, were utilized in sensing of hepatitis C. Detection system exploits the biorecognition between the antibody anti-HCV and the antigenic peptide NS5A-1 through changes in luminescence properties. Films deposition was monitored by UV–vis Absorption and Fluorescence Spectroscopy measurements at each bilayer deposited. The $Eu^{3+}$ luminescence properties were evaluated in the presence of anti-HCV for optical detection of specific antibody and anti-HIV used as negative control. Significant changes in luminescence were observed in the presence of anti-HCV concentrations. A new immunosensor platform is proposed for optical detection of hepatitis C.



## 1. Introduction

Hepatitis C virus (HCV) infects 170 million people worldwide [1,2]. It causes severe liver disease, ranging from chronic hepatitis to cirrhosis and even hepatocellular carcinoma. HCV is an enveloped virus that contains a single-stranded RNA genome of positive polarity. It has been classified within the genus Hepacivirus in the family *Flaviridae*; its uncapped genome is proximately 9600 nucleotides-long [3,4].

Hepatitis C is transmitted by blood, occurring most often through blood transfusions [5]. Contamination can also occur through the use of injecting drugs, accidents with sharp instruments such as needles, scissors, scalpels, blades and toenail pliers when not correctly sterilized, tattoos, piercings, hemodialysis procedures and by sexual contact [6,7].

Several methods for detection of hepatitis C, although quite sensitive, require time, a complex processing of the samples, special equipments, and not rarely, are highly costly [8]. In general, the goal of a detection strategy is the simplicity of the analytical methodology to a practical level and routine, with a minimum demand of operator skills. Thus, detection methods that have performances comparable to traditional have been developed, such as amperometric immunosensors, chemiluminescent, colorimetric as well as optical immunosensors [7–9].

The methods which employ optical immunosensors are based on changes in the optical properties of the system used, by measuring absorption, emission, reflection, scattering, light diffusion, interference, diffraction and refraction [10]. Therefore changes of one or more of the properties: wavelength, amplitude, phase, or polarization are evaluated [11].

Quantum dots (QD), organic luminophores and lanthanide ions containing nanoparticles containing have been used as optical probes materials for biosensors [12]. The current trend in the field of optical biosensors is to develop sensitive devices based on nanostructures and exploring the functionalization of lanthanide ions (such as luminescent probes) to systems for molecular recognition [12,13].

Immobilization of antigenic peptides in nanostructured films has been promising for the development of immunosensors [14,15]. The molecular recognition of antigenic peptide by antibodies leads to selectivity of assays based on immune principles without the requirement to use other complex molecules [16–18]. Recently, our group reported an electrochemical immunosensor for HCV that explores biorecognition between an antigenic peptide (PPLLESWKDPDYVPPWHG) derived from the HCV NS5A-1 protein and anti-HCV [19], where the peptide was immobilized into Layer-by-Layer (LbL) films, alternated with silk fibroin (SF). Using cyclic voltammetry, it was possible to detect the anti-HCV antibody for concentrations between 0.01 and 0.2 μg $mL^{-1}$.

* Corresponding author. Tel.: +55 (16) 33019631.
*E-mail address:* sidney@iq.unesp.br (S.J.L. Ribeiro).

http://dx.doi.org/10.1016/j.jlumin.2015.08.039
0022-2313/

In this work, the molecular recognition of the antibody by the antigenic peptide was performed by photoluminescence spectroscopy measurements. For that $YVO_4$:$Eu^{3+}$ nanoparticles have been used as luminescent markers on nanostructured films for the detection of hepatitis C. The peptide NS5A-1 (PPLLESWKDP-DYVPPWHG) derived from hepatitis C virus (HCV) NS5A protein together with the nanoparticles was immobilized via Layer-by-Layer (LbL) method [20] onto silk fibroin (SF). SF, a biopolymer extracted from natural silk produced by *Bombyx mori*, is a biomaterial that has been widely studied due to the unique combination of mechanical, structural, and biocompatible properties [21–23].

## 2. Materials and methods

### 2.1. Materials

Synthetic peptide NS5A-1 was purchased from Bio-Synthesis Inc. The sequence PPLLESWKDPDYVPPWHG was purified and isolated by HPLC with purity $>90\%$ and sequence confirmed by mass-spectral analysis, as described by Bio-Synthesis Inc. The NS5A-1 solutions were prepared with purified water from Milli-Q system at concentration of 0.5 mg $mL^{-1}$. The antibody specific to HCV (anti-HCV) was obtained from Santa Cruz Biotechnology Inc. Each vial contained 100 μg in 1.0 mL which was diluted in phosphate buffered saline solution (PBS, pH 7.4) solution, in concentrations 0.002 to 1 μg $mL^{-1}$.

### 2.2. $YVO_4$:Eu nanoparticles

Luminescent nanoparticles of $YVO_4$:$Eu^{3+}$ were prepared in two steps following the procedure described in the literature [24,25]. In the first step, sodium orthovanadate ($Na_3VO_4$) was prepared by the reaction of sodium oxide ($Na_2O$) with sodium metavanadate ($NaVO_3$) at 600 °C for 24 h in nitrogen atmosphere [24]. In the second step, aqueous solutions (1 mol $L^{-1}$) of $Y(NO_3)_3$ (9 mL) and Eu $(NO_3)_3$ (1 mL) were mixed in order to obtain a molar ratio Y:Eu=90:10. A volume of 5 mL of sodium citrate solution (2 mol $L^{-1}$) was added to the mixture. A white precipitate (lanthanide citrate) was immediately formed and, still under stirring, 50 mL of $Na_3VO_4$ solution (0.2 mol $L^{-1}$) were added. The reaction medium became transparent and was stirred and heated to 60 °C for 45 min leading to the formation of nanoparticles of $YVO_4$:$Eu^{3+}$ stabilized by citrate ions. Subsequently the solution was cooled and dialyzed against Milli-Q water for 72 h [25].

A nanoparticles suspension with concentration 0.1 mmol $L^{-1}$ was used for the preparation of the LbL films. The nanoparticles suspension was mixed with the peptide solution, forming a single solution in 1:1 volume/volume with a final concentration of 0.1 mmol $L^{-1}$ for the nanoparticles and 0.5 mg $mL^{-1}$ for the peptide.

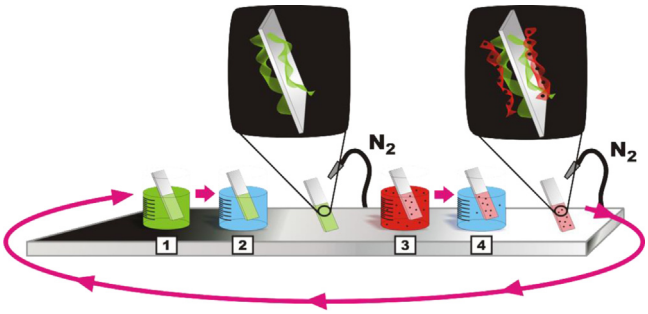


**Fig. 1.** The technical procedure LbL (Layer by Layer). 1 and 3 represent, respectively, the SF solution and the NS5A-1+$YVO_4$:$Eu^{3+}$ nanoparticles solution. 2 and 4 represent Milli-Q water used for washing and removal of weakly adsorbed molecules.

### 2.3. Silk fibroin (SF)

10 g of cocoons were boiled during 30 min in 2 L of the 0.02 mol $L^{-1}$ $Na_2CO_3$ solution in order to remove the sericin. For each 10 g of the silk yarn 100 mL of $CaCl_2/CH_3CH_2OH/H_2O$ (1:2:8) solution were added and the solution heated at 60 °C for dissolution. This solution was then dialyzed against Milli-Q water using a cellulose acetate membrane at room temperature for 48 h. After this procedure, SF was centrifuged three times at 20,000 rpm for 30 min at room temperature to remove impurities and aggregates and was stocked at 5 °C [26]. The concentration of SF in the final solution was 4% in weight. For the preparation of the LbL films SF-NS5A-$YVO_4$:$Eu^{3+}$ the SF solution was diluted to 0.1% (weight/volume).

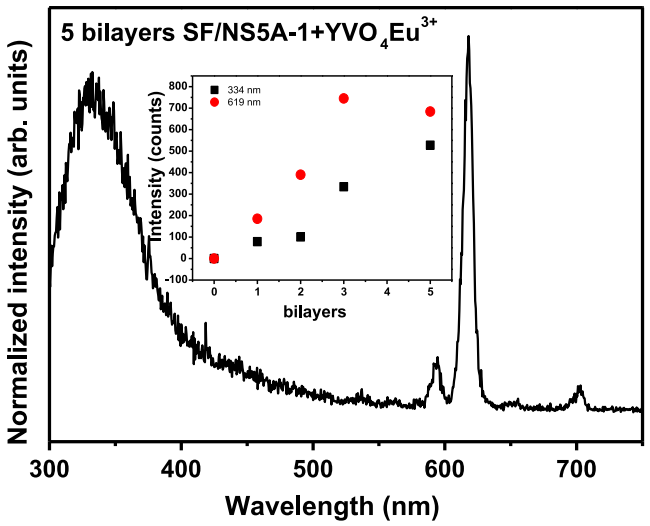


**Fig. 2.** Photoluminescence spectrum (LbL film containing 5 bilayers of SF/NS5A-1+$YVO_4$:$Eu^{3+}$ nanoparticles; $\lambda_{EXC}$=280 nm). Inset: increase of the emission at 334 nm (characteristic of SF and NS5A-1) and 619 nm (characteristic of nanoparticles $YVO_4$:$Eu^{3+}$) for the LbL obtained films as a function of the number of deposited layers.

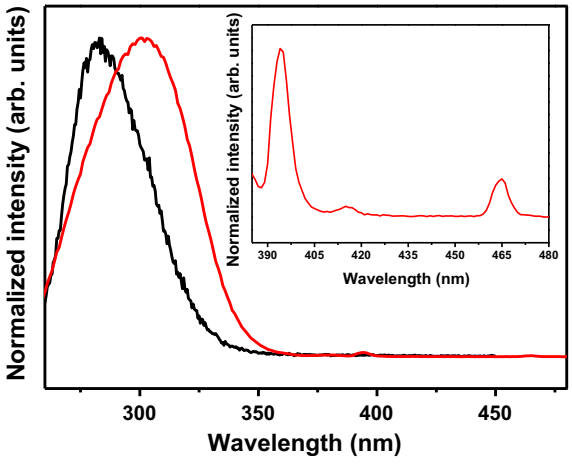


**Fig. 3.** PLE spectrum of the LbL film containing 5 bilayers fibroin/NS5A-1+nanoparticles of $YVO_4$:$Eu^{3+}$ (black curve) and PLE spectrum of the aqueous suspension of $YVO_4$:$Eu^{3+}$ nanoparticles. Inset – zoom of the spectral region from 385 to 480 nm (red curve). (For interpretation of the references to color in this figure legend, the reader is referred to the web version of this article.)

### 2.4. Immobilization of SF/NS5A-1+ $YVO_4:Eu^{3+}$ by Layer-by-Layer method

The films were deposited onto quartz substrates previously treated with a 1:1:5 solution of $NH_4OH:H_2O_2:H_2O$ for 10 minutes at 70 °C, and then with a 1:1:6 solution of $HCl:H_2O_2:H_2O$ for 10 minutes at 70 °C. The deposition of the films on quartz substrates was conducted using the LbL method, Fig. 1. The substrate was immersed in SF solution 0.1% for 10 minutes and in NS5A-1+$YVO_4:Eu^{3+}$ nanoparticles solution 0.5 mg $mL^{-1}$ for 10 min. After each step of deposition the film was washed with Milli-Q water to remove poorly adsorbed molecules and dried gently with flow nitrogen. By repeating this procedure, the desired number of SF/NS5A-1+$YVO_4:Eu^{3+}$ nanoparticles layers could be obtained. All the experiments were performed at room temperature.

### 2.5. Luminescence

The luminescence study was based on the photoluminescence excitation (PLE) and photoluminescence (PL) spectra recorded at room temperature (300 K) using Horiba Jobin Yvon fluorometer (Spex Fluorolog-3) in front face data collection mode (22.5), with a 450 W Xenon lamp as the excitation source coupled to a SPEX-Fluorolog 3 spectrometer with 0.22 nm double monochromators. Slits of 0.5 nm were currently used in all spectra.

## 3. Results and discussions

### 3.1. Immobilization of SF/NS5A-1+ $YVO_4:Eu^{3+}$

Fig. 2 shows the PL spectrum obtained under 280 nm excitation for a film containing 5 bilayers of SF (immobilization matrix) and NS5A-1+$YVO_4:Eu^{3+}$ nanoparticles. A broad emission band is observed peaking at 334 nm and assigned to the fibroin and peptide luminescent amino acid residues (tyrosine and tryptophane). Narrower bands observed in the range of 570–710 nm region were assigned to $Eu^{3+}$ 4f–4f transitions arising from the $^5D_0$ excited state to the $^7F_J$ manifold ($J$=0, 1, 2, 3 and 4). The inset shows the film growth in accordance with each deposited layer, following the emission maximum of the fibroin and peptide band at 334 nm and the $Eu^{3+}$ one at 619 nm. The almost linear behavior observed for the 334 nm band indicates that the nanoparticles do not alter the growth of SF/NS5A-1 LbL film. Concerning the 619 nm the linear increase is due to the adsorption of nanoparticles at each layer deposited.

Fig. 3 shows the PLE spectrum of the 5 bilayers film with the emission being monitored at 619 nm. A broad band is observed ranging from 250 to 350 nm and peaking at around 280 nm. Fig. 3 also shows the PLE spectrum obtained for an aqueous suspension of $YVO_4:Eu^{3+}$ nanoparticles. Characteristic $Eu^{3+}$ narrow bands are observed in the range of 350 nm to 470 nm with the two main bands at 394 nm ($^7F_{0,1}\rightarrow{}^5L_6$) and 464 nm ($^7F_{0,1}\rightarrow{}^5D_2$). This $Eu^{3+}$ bands region is zoomed in the inset for clearer observation. A broader band is observed peaking at around 300 nm, assigned to a composition of the $O^{2-}Eu^{3+}$ and the $O^{2-}V^{5+}$ charge transfer states, which efficiently populate the $Eu^{3+}$emitting states [27,28]. Just the broad band is observed for the composite film suggesting that the $Eu^{3+}$ emission is efficiently excited through the already mentioned charge transfer states together with the aromatic amino acids present in the medium and which absorption occurs at that spectral region. This efficient antenna mechanism is mostly due to the resonance involving amino acids excited states and $O^{2-}Eu^{3+}$ and the $O^{2-}V^{5+}$ charge transfer states since the direct excitation of $Eu^{3+}$ by tyrosine or triptophane amino acids is known to be rather inefficient [29]. This antenna effect will in fact present a key hole in the sensing properties presented hereafter.

### 3.2. Optical detection

Sensing measurements were carried out in the presence of different contents of anti-HCV antibody. The specific interaction antigen-antibody in the nanostructured films is represented schematically in Fig. 4. Solutions of anti-HIV antibody were used in order to check for false-positive tests.

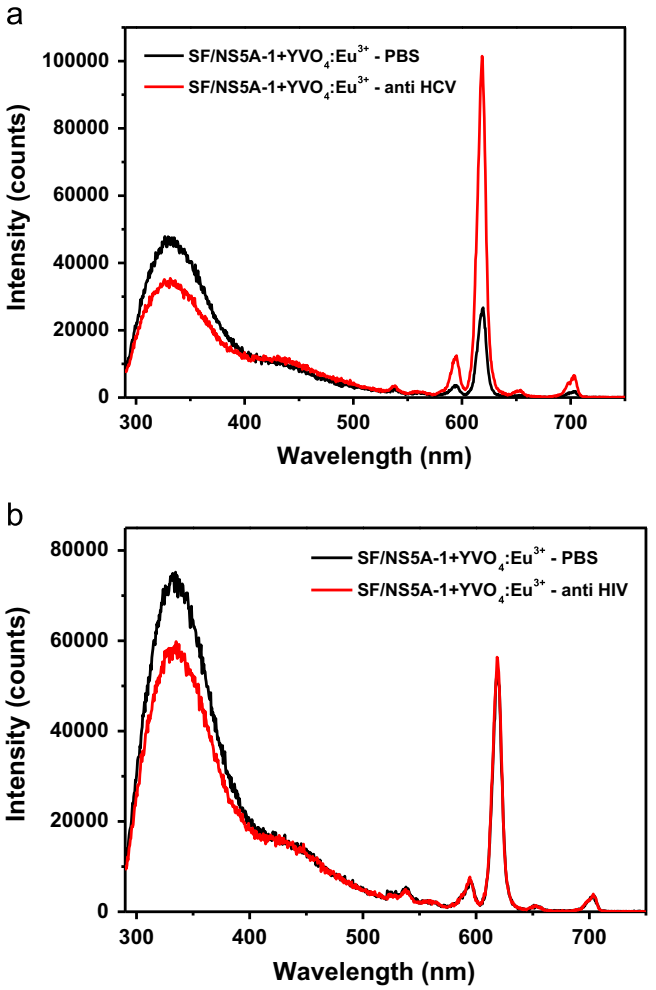


**Fig. 5.** PL spectra of 5 bilayers films in the presence of (a) anti-HCV and (b) anti-HIV. Black curves in PBS and red curves in the presence of the antibodies. (For interpretation of the references to color in this figure legend, the reader is referred to the web version of this article.)

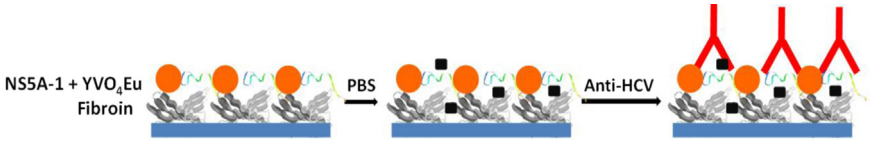


**Fig. 4.** Schematic representation of the LbL film SF/NS5A-1+$YVO_4:Eu^{3+}$nanoparticles showing specific recognition in the presence of anti-HCV antibodies.

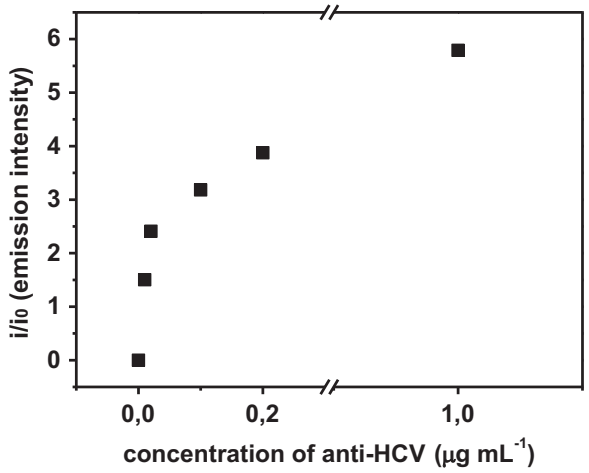


**Fig. 6.** $Eu^{3+}$ 619 nm normalized emission intensity ($I/I_0$, where $I_0$ is the initial PL intensity in the absence of the antibody) as a function of the anti-HCV concentration.

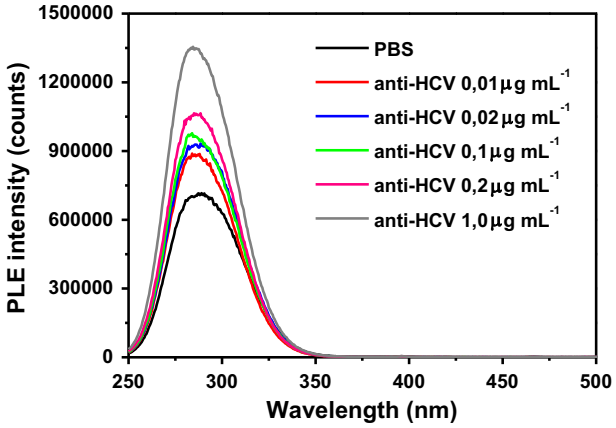


**Fig. 7.** PLE spectra obtained for the LbL film containing 5 bilayers of fibroin/NS5A-1+nanoparticles $YVO_4$:$Eu^{3+}$ in the presence of different concentrations of anti-HCV.

PBS solutions with anti-body concentrations 0, 0.01, 0.02, 0.1, 0.2 and 1 μg $mL^{-1}$ were used. Fig. 5(a) shows PL spectra of the film in the absence and presence of anti-HCV antibodies. When no antibody is present the spectrum shows the broad emission due to the SF and NS5A-1 at about 330 nm and the narrow $Eu^{3+}$ bands. The spectrum is dominated by the broad band. When anti-HCV was added the adsorption of anti-HCV antibodies through specific recognition of the antigen lead to a relative increase for the $Eu^{3+}$ emission at 619 nm. Fig. 5(b) shows spectra obtained upon addition of anti-HIV. No enhancement is observed confirming the specificity of the optical detection for hepatitis C.

The mechanisms for antigen-antibody interaction and the energy transfer process anti-HCV→sensing film are still unclear. Nevertheless the PL intensity increases with the anti-HCV concentration. Fig. 6 shows the PL intensity (normalized by the PL intensity observed in the absence of the antibody) as a function of the anti-HCV content and in fact an asymptotic behavior is observed, showing a limiting value. The curve indicates the emission increases with increasing concentration of anti-HCV in the range of 0 to 0.01 μg $mL^{-1}$, that is, the antibody can be detected even at low concentrations. Above that concentration value, a tendency to saturation is observed indicating most probably that all recognition sites were probably filled.

The same behavior was observed before for electrochemical similar sensors [19]. Interesting enough a multifunctional behavior is observed. The nanostructured films could be used in both electrochemical and optical detection.

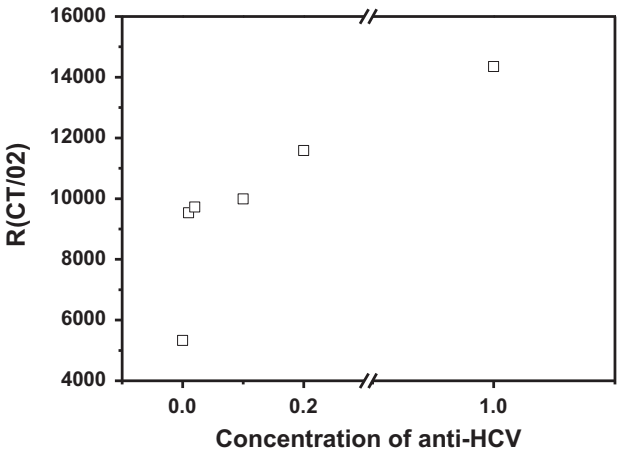


**Fig. 8.** Intensities ratio between the broad band at 280 nm and the ff transition at 464 nm in PLE spectra as a function of the antibody concentration.

Fig. 7 shows PLE as a function of the concentration of anti-HCV. The relative increase in the excitation band intensity confirms the increasing efficiency of energy transfer process from the anti-HCV amino acids to the vanadate nanoparticles. Most probably, the increasing number of tryptophan and/or tyrosine amino acids at the neighborhood of $Eu^{3+}$ ions leads to the increasing PL intensity.

Fig. 8 shows the relative increase observed for the broad excitation band. It shows the evolution of the intensities ratio between the broad band at 280 nm and the intrinsic $Eu^{3+}$ band at 464 nm (which is rather observed in Fig. 7 due to low intensity) with the anti-HCV concentration The pronounced emission intensity and the sensitivity to low anti-HCV concentration allow proposing these nanostructured films as a new luminescent sensing platform.

## 4. Conclusions

Self-assembled LbL films composed of silk fibroin as immobilization matrix for the NS5A-1 (HCV) peptide together with $YVO_4$:$Eu^{3+}$ nanoparticles have been used to identify anti-HCV macromolecules in solution.

An efficient energy transfer process involving amino acids tyrosine and triptophane, present in both antigenic peptide and anti-body, and the nanoparticles vanadate groups lead to enhanced $Eu^{3+}$ emission. Specificity was tested by using anti- HIV as a probable false-positive target. Moreover these new optical immunosensors can be easily processed in low-cost devices by using UV-LEDs and visible photodetectors.

## Acknowledgments

This work was supported by Brazilian funding agencies CNPq and FAPESP and also Nanobiotec-CAPES network (Brazil).

## References

[1] K. Bornschlegel, D. Holtzman, R.M. Klevens, J.W. Ward, Morb. Mortal. Wkly. Rep. 62 (2013) 357.
[2] B. Hajarizadeh, J. Grebely, G.J. Dore, Nat Rev., Gastroenterol. Hepatol. 10 (2013) 553.

[3] C.M. Fauquet, A. Mayo, J. Maniloff, U. Desselberger, L.A. Ball, Virus Taxonomy: Report of the International Committee on Taxonomy of Viruses, 8th ed., Elsevier Science, London, 2005.
[4] B.D. Lindenbach, C.M. Rice, Nature 436 (2005) 933.
[5] Y.J. Grebely, G.V. Matthews, G.J. Dore, Nat Rev., Gastroenterol. Hepatol. 8 (2011) 265.
[6] J.Y. Jang, R.T. Chung, Gut Liver 5 (2011) 117.
[7] R.A. Tohme, S.D. Holmberg, Hepatology 52 (2010) 1497.
[8] D.R. Gretch, Hepatology 26 (1997) S43.
[9] D.B. Strader, T. Wright, D.L. Thomas, L.B. Seeff, Hepatology 39 (2004) 1147.
[10] S.C.L. Pinheiro, I.M. Raimundo Jr, Quím. Nova 28 (2005) 932.
[11] A. Brecht, G. Gauglitz, Biosens. Bioelectron. 10 (1995) 923.
[12] S.V. Eliseeva, J.-C.G. Bunzli, Chem. Soc. Rev. 39 (2010) 189.
[13] A. De La Escosura-Muñiz, C. Parolo, A. Merkoçi, Mater. Today 13 (2010) 24.
[14] N.J. Ronkainen, H.B. Halsall, W.R. Heineman, Chem. Soc. Rev. 39 (2010) 1747.
[15] F.R.R. Teles, L.P. Fonseca, Mater. Sci. Eng. C 28 (2008) 1530.
[16] J. Rickert, W. Göpel, W. Beck, G. Jung, P. Heiduschka, Biosens. Bioelectron. 11 (1996) 757.
[17] Y. Yuan, J. Zhang, H. Zhang, X. Yang, Analyst 137 (2012) 496.
[18] L. Petri, M. Ferreira, M.L. Moraes, J. Nanosci. Nanotechnol. 11 (2011) 6705.
[19] M.L. Moraes, L.R. Lima, R.R. Silva, M. Cavicchioli, S.J.L. Ribeiro, Langmuir 29 (2013) 3829.
[20] G. Decher, Science 277 (1997) 1232.
[21] F.G. Omenetto, D.L. Kaplan, Science 329 (2010) 528.
[22] C.-Z. Zhou, F. Confalonieri, M. Jacquet, R. Perasso, Z.-G. Li, J. Janin, Proteins 44 (2001) 119.
[23] C.-Z. Zhou, Nucl. Acids Res. 28 (2000) 2413.
[24] M.G. Barker, A.J. Hooper, J. Chem. Soc. Dalton Trans. 15 (1973) 1513.
[25] D. Giaume, V. Buissette, K. Lahlil, T. Gacoin, J.P. Boilot, D. Casanova, E. Beaurepaire, M.P. Sauviat, A. Alexandrou, Prog. Solid State Chem. 33 (2005) 99.
[26] D.N. Rockwood, R.C. Preda, T. Yücel, X. Wang, M.L. Lovett, D.L. Kaplan, Nat. Protoc. 6 (2011) 1612.
[27] A. Huignard, V. Buissette, A.C. Franville, T. Gacoin, J.P. Boilot, J. Phys. Chem. B 107 (2003) 6754.
[28] A. Szczeszak, T. Grzyb, Z. Sniadecki, N. Andrzejewska, S. Lis, M. Matczak, G. Nowaczyk, S. Jurga, B. Idzikowski, Inorg. Chem. 53 (2014) 12243.
[29] A.M. Reynolds, B.R. Sculimbrene, B. Imperiali, Bioconjug. Chem. 19 (2008) 568.